Numerical Simulation of Flow Separation Control over a Hump Using DBD Plasma Actuator

A. Jahangirian*, R. Khoshkhoo**
***,** Aerospace Engineering Department, Amirkabir University of Technology, Tehran, Iran**

Keywords: *Turbulent flow; Flow Control; Dielectric Barrier Discharge Actuator; Numerical Simulation; Hump model*

Abstract

A numerical simulation method is employed to investigate the effect of the steady and unsteady plasma body forces on the flow field over a hump model. The plasma body forces created by single Dielectric Barrier Discharge (DBD) plasma actuators were modeled with a phenomenological plasma method coupled with 2-dimensional compressible turbulent flow equations. Turbulence models based on $k-\epsilon$ two-equations are investigated. The body force distribution is assumed to vary linearly in the triangular region around the actuator, and the body force decreases by moving away from the surface. The equations are solved using an implicit finite volume method on unstructured grids. In this paper, the responses of the separated flow field to the effects of single DBD plasma actuator in steady and unsteady modes are studied. The effects of the plasma actuator positions on the flow field are also investigated. It is shown that the $k-\epsilon$ turbulence model do an accurate prediction for the overall features of the flow field and the DBD employment has significant effects on turbulent flow separation control over the hump.

1 Introduction

Flow separation is an undesirable phenomenon which causes loss of lift force, increases drag force and produces control problems for different aerospace vehicles. The solution of this problem is thus highly demanded in fluid dynamics researches [1].

Different methods for flow separation control including active and passive techniques have been carried out. Active separation control techniques have benefits of passive techniques without their disadvantage in off-design conditions [2].

Dielectric Barrier Discharge (DBD) plasma actuator is one of the active flow control devices that have been successfully used in aerodynamic flow control applications. Thus, considerable researches have been carried out on DBD plasma actuators over the past decade [3].

DBD plasma actuator has distinctive potentials such as reduction in size, weight and drag, increasing reliability, low cost, no moving parts, wide frequency bandwidth, rapid on-off capability, low energy consumption, increasing stealth, without bumps or gaps over the airfoil surface, and low power input. The schematic of the DBD plasma actuator is shown in Fig. 1.

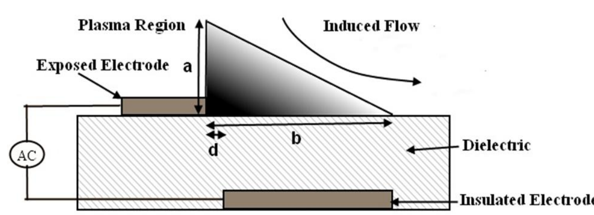

Fig. 1. Diagram of a DBD plasma actuator and its effective region.

DBD plasma actuator operates in either steady or unsteady mode. The interesting point about the unsteady mode of the DBD actuator is that the input energy consumption in unsteady mode is less than steady mode. In this study, the DBD actuator in the operational steady and unsteady modes is assumed.

First-principles-based modeling and phenomenological modeling are two approaches for simulation of the DBD plasma actuator. The phenomenological approach in comparison with the first-principle-based modeling approach cannot definitely predict the plasma physics, but it is rather simple and very appropriate for simulation of the effects of plasma on the fluid. Full description about both approaches is presented by Jayaraman and Shyy [4].

The Shyy model is one of the well-known models from the phenomenological modeling approach that is employed to simulation of different fluid dynamics problems and its results are compared with the experimental data in the study by Jayaraman and Shyy [5].

In this model, the effect of the plasma actuator on the fluid flow is assumed as a body force in the triangular region with the dimensions of a and b (see Fig. 1). In this region, the electric field is linearized and its lines are parallel except in the small region near the cathode. Additionally, as the distance from the cathode increases, the strength of the electric field lines decreases [4].

He and others simulated $k-\epsilon$, $k-\omega$ and S-A turbulent models using fluent. They showed that the DBD plasma actuator could be effective in controlling the turbulent flow separation over the hump [6].

Yakeno and others solved the two dimensional Navier-Stokes equations for flow separation control over hump by the DBD plasma actuator in low Mach number and low Reynolds number conditions. They showed that the DBD plasma actuator can increase reattachment by increasing turbulence fluctuation and modifying the momentum transfer [7]. Also, the separation location is not sensitive to Reynolds number in this model [8]. The considerable researches have been carried out on the wall-mounted hump model [9, 10].

In the present study, the two dimensional Reynolds-averaged Navier-Stokes equations are used for numerical simulation over the hump model. The flow is assumed turbulent. The effect of DBD plasma actuator in steady and unsteady modes for flow separation control around a simple the wall-mounted hump in subsonic flow and high Reynolds number is investigated. The results of with and without control are compared with experimental data [8] on the hump model.

2 Computational Method

2.1 Governing flow equations

In this study, two-dimensional unsteady compressible Navier-Stokes equations are employed to describe the flow field, which is augmented by source terms representing the plasma forcing of the DBD actuator. The flow equations can be written in the general and conversation form in a Cartesian coordinate system as follows:

$$\frac{\partial X}{\partial t}+\frac{\partial F_I}{\partial x}+\frac{\partial G_I}{\partial y}=\frac{\partial F_V}{\partial x}+\frac{\partial G_V}{\partial y}+S \qquad (1)$$

Where, $X=\{\rho,\rho u,\rho v,\rho e\}$ is the vector of dependent variables. The terms F_I and G_I are the convective fluxes, and F_V and G_V are the diffusion fluxes. The term S is the source vector including the plasma force which is described with more details in the next section. The convective and diffusive flux vectors can be written as follows:

$$F_I=\begin{bmatrix}\rho u\\ \rho u^2+p\\ \rho uv\\ (\rho e+p)u\end{bmatrix} G_I=\begin{bmatrix}\rho v\\ \rho uv\\ \rho v^2+p\\ (\rho e+p)v\end{bmatrix} \qquad (2)$$

$$F_V=\begin{bmatrix}0\\ \tau_{xx}\\ \tau_{yx}\\ (u\tau_{xx}+v\tau_{xy})+K\dfrac{\partial T}{\partial x}\end{bmatrix}$$

$$G_V=\begin{bmatrix}0\\ \tau_{xy}\\ \tau_{yy}\\ (u\tau_{xy}+v\tau_{yy})+K\dfrac{\partial T}{\partial y}\end{bmatrix} \qquad (3)$$

Where ρ, p, t, e, T and K represent the density, pressure, time, total energy per unit value, temperature and heat conduction coefficient, respectively. u and v are the velocity vector components in x and y directions, respectively. $\tau_{yy}, \tau_{xx}, \tau_{xy}$ and τ_{yx} are stress tensor components. All mentioned values are non-dimensional based on the following scaling:

$$\rho^*=\frac{\rho}{\rho_{ref}}, U^*=\frac{U}{\frac{a_{ref}}{\sqrt{\gamma}}}=\frac{U}{\sqrt{\frac{p_{ref}}{\rho_{ref}}}}, p^*=\frac{p}{p_{ref}}, \qquad (4)$$

$$e^* = \frac{e}{\frac{p_{ref}}{\rho_{ref}}}, \mu^* = \frac{\mu}{\mu_{ref}} \frac{M\sqrt{\gamma}}{Re}, T^* = \frac{T}{T_{ref}}$$

where the subscript ref and superscript * denote the reference and non-dimensional values, respectively. U, μ , γ and a_{ref} represent the velocity vector, the molecular viscosity coefficient, ratio of specific heats and sound speed, respectively. Non-dimensional parameters Re and M denote the Reynolds number and the Mach number, respectively. The perfect gas is assumed, and the Sutherland law is used to calculate the molecular viscosity coefficient. In this study, the flow is assumed turbulent. The $k-\epsilon$ model is used for calculation of the flow [11].

2.2 DBD actuator modeling

The source term vector in equation (1) is written as follows:

$$S = \begin{bmatrix} 0 \\ D_c \rho_c E_x A(t) \\ D_c \rho_c E_y A(t) \\ \beta D_c A(t)(uE_x + vE_y) \end{bmatrix} \quad (5)$$

Where E_x, E_y are the components of electric field vector in the Cartesian system. ρ_c is the charge number density and *A(t)* is a parameter between 0 and 1 that shows the strength of the actuator in unsteady mode, β is the parameter either 0 or 1, which is used to show the effect of the energy produced and work done by body force. Actually, the work done by plasma force is very small, so β is assumed to be zero in this study. D_c is the non-dimensional plasma force magnitude parameter, which is defined as:

$$D_c = \frac{\rho_{c,ref} e_c E_{ref} L_{ref}}{P_{ref}} \quad (6)$$

In this equation, e_c denotes the electronic charge (electrons) and L is the chord length of the airfoil. In this study, the Shyy model is employed to simulate the effect of plasma force on the flow field. In this model, it is assumed that the plasma region is a triangular area in the down-stream of the exposed electrode on the dielectric layer. Also, it is assumed that the extent of the electric field in the plasma region decreases linearly along with the direction axes.

Plasma body force is assumed in steady and unsteady modes. In unsteady mode, duty cycle, starting time of actuation are important. More details about the Shyy model are described in references [4, 12, 13]. Also, the values of $\rho_c = 10^{11}/cm^3$, $\Delta t = 67\mu s$ and $D_c = 2.5$ are set. The frequency is assumed $1kHz$. The length and height of triangular area are 0.02 and 0.01 of the hump length respectively. In unsteady mode, the duty cycle of 20% and inter-pulse of 0.7 of total time period (T_c) are considered.

2.3 Numerical flow solution method

Two-dimensional compressible Navier-Stokes equations are applied as the governing flow equations. The $k-\epsilon$ turbulence model is used for turbulent flow simulation.

The flow field is unsteady and the mean values of the flow variables are obtained by averaging the instantaneous values over several time periods. A cell-center implicit finite-volume method is employed following the work of Jahangirian et al [14] to discretize the governing equations. The artificial dissipation terms are added to the main flow equations for numerical stability reasons. So a semi-discrete form of the Navier-Stokes equations is represented as:

$$\frac{d}{dt}(Q_i A_i) + R_i(Q) - D_i(Q) = 0 \quad (7)$$

Where $R_i(Q)$ denotes the convective and viscous fluxes, A_i is the area of the cell and $D_i(Q)$ is the artificial dissipation flux. The artificial dissipation terms provide background dissipation to suppress odd-even modes using a blend of first and third-order dissipative terms.

In this study, residual smoothing and the explicit four stages Runge-Kutta method are applied. The CFL number of 100000 is used for the implicit algorithm and convergence error (10^{-8}) is considered and the explicit CFL number of 4 and convergence error (10^{-2}) is used.

For viscous flows, no-slip boundary conditions were imposed. Non-reflecting boundary conditions are also used in the far-field based on the characteristic method.

In this study, a wall-mounted hump model is used for simulation of canonical turbulent separated flow field. It is concluded a relatively long fore-body and a short separation concave ramp near the aft part of the model.

The flow configuration and boundary conditions of hump model are exhibited in Fig. 2. The chord length of hump and the chord of span are 420 mm and 356 mm respectively. The maximum height of the hump model is 53.7 mm. the inlet is located at $x/c = 2.14$. The outlet is located at $x/c = 4.0$. the outlet pressure is set at $p/p_{ref} = 0.99962$ by increase high of outlet. The top-wall is located at $x/c = 0.9$. In all simulations, the Reynolds number 929000 and Mach number 0.1 are considered.

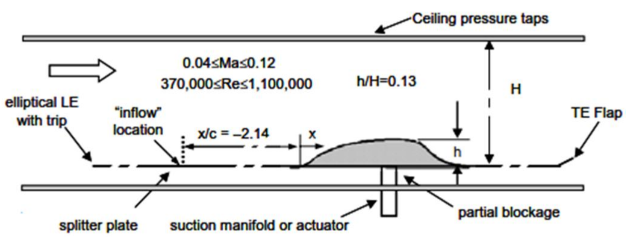

Fig. 2. The flow configuration and boundary conditions of hump model [6].

In this study, an unstructured grid is generated around hump model. The grid contains stretched high aspect ratio triangular cells inside the viscous layer and wake region while using isotropic cells outside these regions (Fig. 3). Total number of cells is approximately 17520 cells. 218 points are placed on the surface of the hump model. The vertexes are concentrated close to the plasma actuator location on the hump model. The normal distance of the first node from the concave ramp is taken equal to 0.001 of the chord length for $k-\epsilon$ turbulent model. The number of grid point is 283×31 ($x \times y$) in Cartesian coordinate.

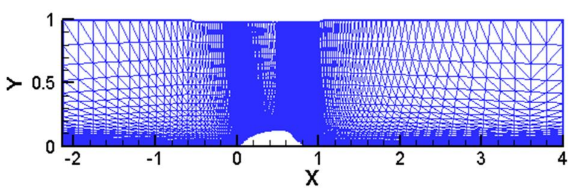

Fig. 3. Unstructured generated viscous grid

3 Results

3.1 Without control condition

The surface pressure coefficient ($\boldsymbol{C_p}$) and the skin friction coefficient ($\boldsymbol{C_f}$) in without control condition are shown in Fig. 4, which are compared with experimental results [8].

The results show that the $k-\epsilon$ turbulence model does a reasonable prediction for the overall features of the flow field and this model has the high accuracy in flow separation simulation in comparison with experimental data.

Fig. 4(a) show that the pressure coefficient decrease downstream of the hump leading edge and it increases up to 0.66 of the hump chord length, then it decrease sharply due to flow separation and reattach flow in downstream of the trailing edge. The results show the less reduction of pressure level than experimental data in two separation locations.

The skin friction coefficient is shown in Fig. 4(b), which is compared with experimental data. The separation point is identified with high accuracy by using the $\boldsymbol{k-\epsilon}$ turbulent model.

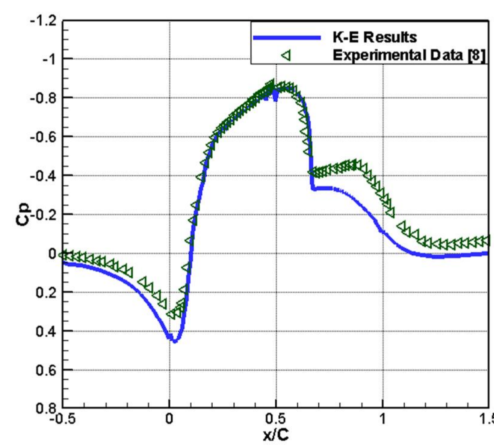

a) Surface pressure coefficient

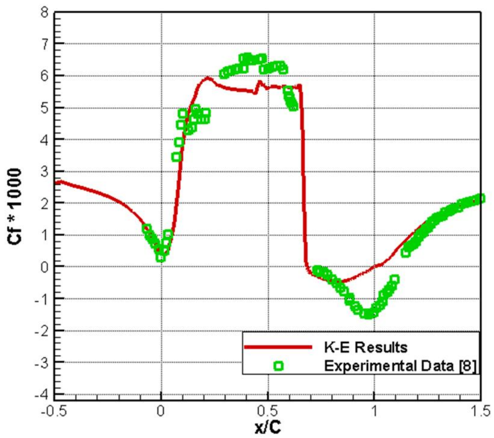

b) Surface skin friction coefficient

Fig. 4. The Surface pressure and skin friction coefficients in without control condition, Re=929000, M=0.1

3.2 With control condition in steady mode

The DBD plasma actuator is located at 0.66 of the hump chord length. The surface pressure coefficient (C_p) and the skin friction coefficient (C_f) in with-control condition are shown in Fig. 5, which are compared with without-control condition. The results show that the plasma actuator makes a sharp reduction of pressure level in plasma actuator location and the DBD plasma actuator reduce the flow separation. The skin friction coefficient in Fig. 5 b) shows that the DBD plasma actuator has effect over reattachment of flow, and doesn't affect over separation point, the reattachment location is moved from 1.1 to 1 chord of length.

The stream lines colored by U-velocity for with control condition and without control condition are exhibited in Fig. 6. It is visible that then separation area decrease in with-control condition and circulation area decrease.

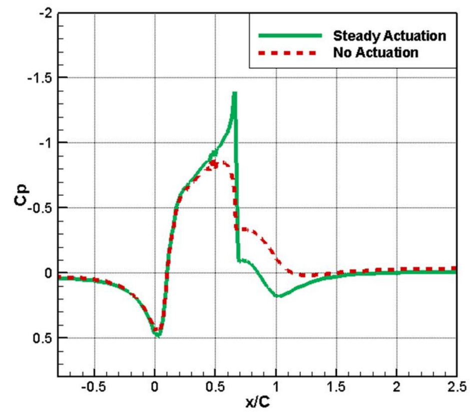

a) Surface pressure coefficient (C_p)

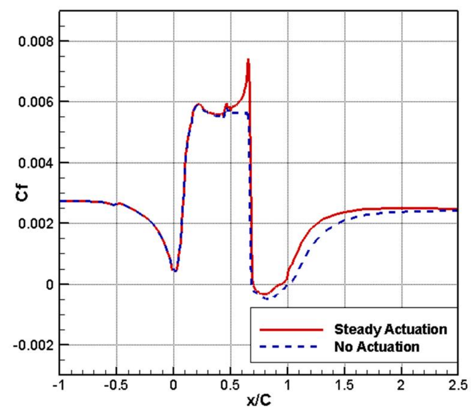

b) Skin friction coefficient(C_f)

Fig. 5. The Surface pressure and skin friction coefficients in with control condition, Re=929000, M=0.1

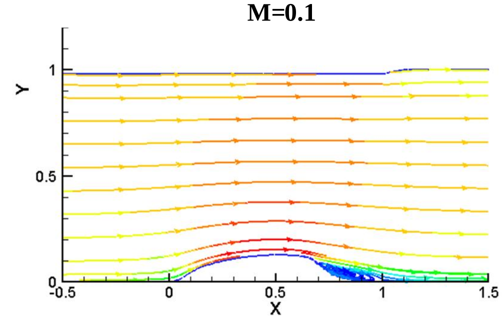

a) Without control condition

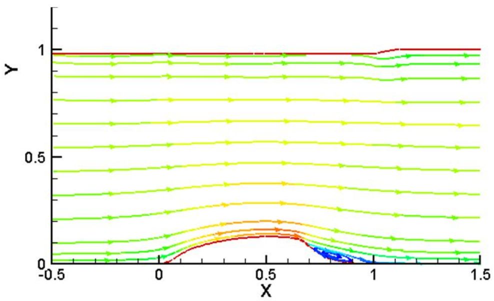

b) With-control condition

Fig. 6. The streamlines colored by U-velocity, Re=929000, M=0.1

3.3 With control condition in unsteady mode

The DBD plasma actuator is located at 0.66 of the hump chord length in unsteady mode. The surface pressure coefficient and the skin friction coefficient in with-control condition in unsteady mode are shown in Fig. 7, which is compared with the results of steady mode. This results show that the DBD plasma actuator in unsteady mode can decrease separation and circulation area as same as steady mode with low input energy consumption.

Figure 8 shows the stream lines colored by U-velocity in steady and unsteady modes. The reattachment locations are 1 chord of length in both modes.

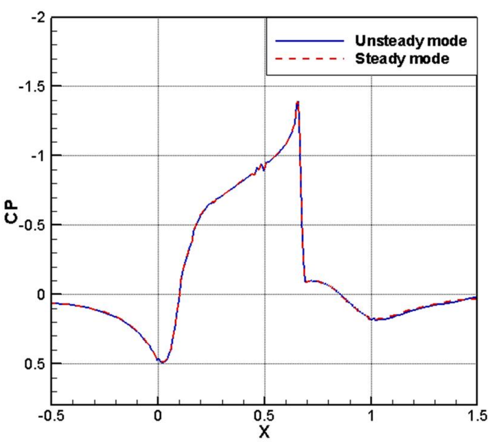

a) Surface pressure coefficient

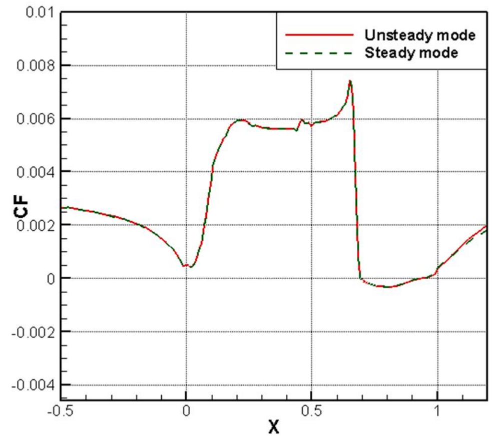

b) Skin friction coefficient

Fig. 7. The surface pressure and skin friction coefficients in with control condition in steady ad unsteady modes, Re=929000, M=0.1.

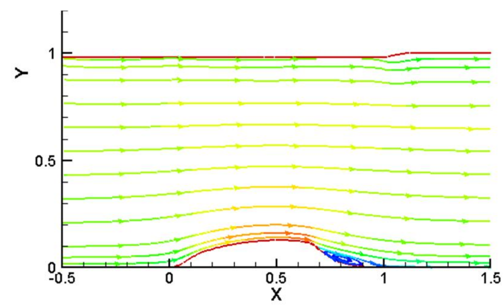

a) Steady mode

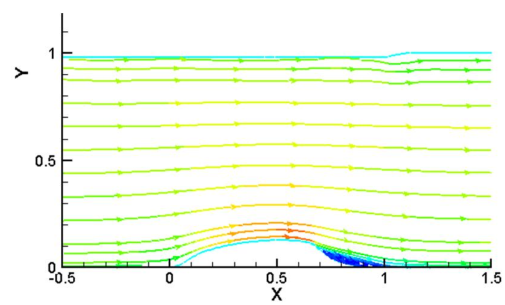

b) Unsteady mode

Fig. 8. U-velocity contours in with control condition, Re=929000, M=0.1

3.4 The effect of plasma actuator location

The effect of the plasma actuator location on the flow characteristics is exhibited in Fig. 9. This Fig. shows the surface pressure distribution when plasma actuator is placed after and before separation point from 0.63 to 0.7 of the chord length. The results show that, if plasma actuator places down-stream of the separation point. By increasing the distance between plasma actuator location and the separation point, the separation will not decrease. Also, if plasma actuator places upstream of the separation point. By increasing the distance between plasma actuator location and the separation point, the separation will not decrease.

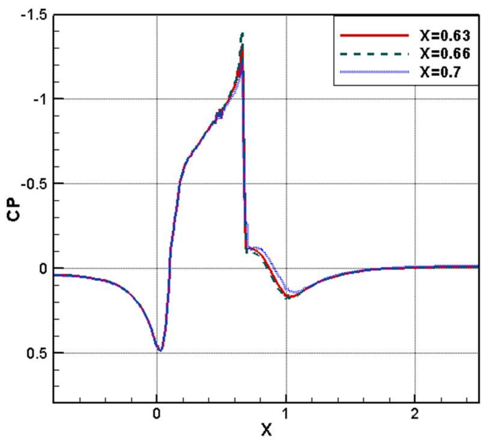

Fig. 9. The Surface pressure coefficient by changing plasma actuator location in with control condition in steady mode, Re=929000, M=0.1.

4 Conclusions

The effect of plasma body force on the flow field over hump model at the Reynolds number of 929000 and Mach number of 0.1 was simulated. Plasma body force was formed by the single DBD actuators in steady and unsteady modes. Two-dimensional unsteady compressible Navier-Stokes equations were employed. The $\boldsymbol{k-\epsilon}$ turbulence model is used for flow simulation. The Shyy model was used to simulate the plasma body force. In this paper, the effect of plasma actuator in steady and unsteady modes and the effect of plasma actuator in different locations on flow separation control were studied.

The results showed that the $k-\epsilon$ turbulence model does an accurate prediction for the overall features of the flow field and this turbulent model has the high accuracy in flow separation simulation.

The DBD employment has significant effects on turbulent flow separation control over the hump in steady and unsteady modes. The unsteady mode has the same effect on flow separation control with low input energy consumption. Finally, the best location of the plasma actuator is near the separation point.

References

[1] Greenblatt D and Wygnanski I J. The control of flow separation by periodic excitation. *Progress in Aerospace Sciences*, Vol.36, No.7, pp.487–545, 2000.

[2] Little J, Nishihara M, Adamovich I and Samimy M. High-lift airfoil trailing edge separation control using a single dielectric barrier discharge plasma actuator. *Journal of Experiments in Fluids*, Vol. 48, No. 3, pp. 521–537, 2010.

[3] Corke T C, Enloe C L and Wilkinson S P. Dielectric Barrier Discharge Plasma Actuators for Flow Control. *Annual Review of Fluid Mechanics*, Vol. 42, No. 1, Pp. 505–529, 2010.

[4] Jayaraman B and Shyy W. Modeling of dielectric barrier discharge-induced fluid dynamics and heat transfer. *Progress in Aerospace Sciences*, Vol. 44, No.3, Pp.139–191, 2008.

[5] Jayaraman B and Shyy W. Flow Control and Thermal Management Using Dielectric Glow Discharge Concepts. *Proc 33rd AIAA Fluid Dynamics Conference and Exhibit*, Vol. Jun 2003, pp.1-12, 2003.

[6] He C, Corke T C and Dame N. Numerical and Experimental Analysis of Plasma Flow Control over a Hump Model Electrode AC Voltage Source. *Proc 45th Aerospace Sciences Meeting*, Reno, Nevada, pp.1–16. , January 8-11, 2007.

[7] Yakeno A, Kawai S, Nonomura T and Fujii K. Flow Separation control based on turbulence transition around a two-dimensional hump at different Reynolds numbers. *International Journal of Heat and Fluid Flow*, Vol. 55, Pp. 52–64, 2015.

[8] Greenblatt D, Paschal K, Schaeffler N, Washburn, A, Harris J and Yao C. A separation control CFD validation test case. Part 1: baseline and steady suction. *AIAA Paper* 2004-2220, 2004.

[9] Rumsey C, Gatski T, Sellers W, Vatsa V and Viken S. Summary of the 2004 CFD Validation Workshop on Synthetic Jets and Turbulent Separation Control. *AIAA Paper*, No. 2004-2217, 2004.

[10] Cappelli D and Mansour N. Performance of Reynolds Averaged Navier-Stokes Models in Predicting Separated Flows: Study of the Hump Flow Model Problem. *44th AIAA Thermophysics Conference*, San Diego, CA; United States, Pp. 1–26, 2013.

[11] Wilcox C D. *Turbulence modeling for CFD.* Second Edition, DCW Industries, California, 1998.

[12] Shyy W, Jayaraman B and Andersson A. Modeling of glow discharge-induced fluid dynamics. *Journal of Applied Physics*, Vol. 92, No.11, Pp.6434-6443, 2002.

[13] Gaitonde D, Visbal M and Roy S. A coupled approach for plasma- Based flow control simulations of wing sections, *44th AIAA Aerospace Sciences Meeting and Exhibit*, Reno, Nevada. No. AIAA 2006-1205, 2006.
[14] Jahangirian A and Hadidoolabi M. Unstructured moving grids for implicit calculation of unsteady compressible viscous flows. *International Journal for Numerical Methods in Fluids*, Vol. 47, No. 10–11, Pp.1107–1113, 2005.

Contact Author Email Address

mailto: ajahan@aut.ac.ir

Copyright Statement